

FATIGUE CRACK GROWTH IN FERROELECTRIC CERAMICS DRIVEN BY CYCLIC ELECTRIC FIELD

D.N. Fang, B. Liu and K.C. Hwang
Department of Engineering Mechanics
Tsinghua University, Beijing 100084, China

ABSTRACT

In this paper, fatigue crack propagation of the ferroelectric ceramics with initial penetrated cracks under cyclic electric loading is investigated. The experimental results show that there are two distinct fatigue mechanisms. Under low electric loading, the emergence and growth of microcracks is major mechanism, while under a high electric field, the propagation of the macroscopic crack is dominant. It was found in experiments that the crack growth is in company with electric breakdown occurred inside the crack.

KEYWORDS

Ferroelectric ceramic, Electric Fatigue, Crack propagation, Cyclic loading

INTRODUCTION

Electric-field-induced fatigue refers to the deterioration of material properties associated with electric cycling. Experiments by Uchino and Furuta [1], Jiang and Cross [2], Cao and Evans [3], Lynch et al. [4], Hill et al. [5], Tai and Kim [6], Zhu et al. [7], Winzer et al. [8], have shown that cracks grow in ferroelectric ceramics under cyclic electric field. The performance of ferroelectric ceramics in smart structures is often hampered by crack propagation in the devices [1]. Does the crack grow by electric breakdown, or by the stress field near the crack tip? Based on the experimental observation and the analysis, the present paper provides both a physical mechanism analysis and a mechanistic explanation. In this paper, different from most work done by others, the propagation of an initial penetrated crack in ferroelectric ceramics instead of the growth of initial surface cracks produced by indentation is studied. Note that the surface crack belongs to a three-dimensional crack and there exists residual stress in the neighborhood of the indentation. The major obstacle in introducing a penetrated crack in the specimen is the brittleness of ferroelectric ceramics. On the other hand, considered that the ferroelectrics usually are used in the low electric loading, the authors try to investigate the fatigue behavior in a more wide loading range. It is more important to study the case of fatigue with low cyclic amplitude ($E \leq E_c$).

EXPERIMENTAL PROCEDURE

The specimen is shown in Fig.1. The material used for the experiment was PZT-5, which has a tetragonal crystal structure at room temperature and an average $3 \mu\text{m}$ grain size. Specimens were

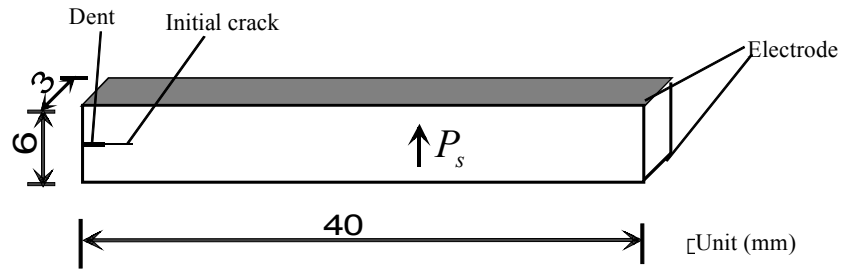


Fig. 1: Schematic of the specimen

cut and polished to dimensions of $40 \times 6 \times 3(\text{mm})$. Gold electrodes were sputtered onto the upper and lower surfaces of the PZT-5 specimen. The specimens were poled in the direction perpendicular to the crack faces under an electric field of $3E_c$ (the coercive field, $E_c = 1000\text{V}/\text{mm}$) at a temperature of 130°C . At first, a short notch with a width of 0.25mm was generated on the specimens. Then, by use of a Combined Load Device that was specially designed for producing pre-crack, the specimens were pre-cracked. For the details of this special technique, one can read the paper of Zhang et al [9]. The specimen was immersed in a silicon oil container that was made of transparent and insulating plexiglass and subjected to a cyclic electric field through the bolts that attach to the electrodes. The sine wave forms were applied to the specimens under a wide amplitude range of $0.8E_c \sim 3.2E_c$. Because the specimen was plated on the upper and lower surfaces, if no crack existed in the specimen, the electric field in the specimen would be uniform. The power used in experiments was a voltage-adjustable alternating high voltage supplier, which can reach its highest output of $\pm 30 \text{ kV}$. There are five available frequencies which are 50 Hz, 4Hz, 3Hz, 2Hz and 1Hz.

RESULTS AND DISCUSSIONS

All specimens were observed through microscopy with 400 times amplification before loading. No obvious microcrack was found and the crack tips were very sharp. Fig. 2 exhibits that a crack propagates from an initial penetrated crack in the specimen. The experimental results [3] and the theoretical explanation [10] showed that there exists the anisotropy of fracture toughness in ferroelectrics. That is, the crack propagates along the direction perpendicular to the electric field more easily than along the direction parallel to the electric field. The reason that the main crack grows along the middle crack surface is due to the fact that the crack in the middle surface would bring the greatest disturbance for the electric and mechanical field. This may cause the strongest electric field and stress concentrations that induce the largest energy release rate.

In the test, it was also found that the crack did not grow at once when the electric field was applied. It always frizzed for some time, then propagated quickly, especially under a low electric field. Moreover, there were some phenomena that occur before the crack grows. For example, some little bubbles produced from the main crack and the buzz noise can be heard. When the loading frequency was low, it can be found that sparks occurred inside the crack, and some black powder appeared on the crack faces. After a period of fatigue cycling, detached the specimen along the crack, we found that the crack surface generated by electric-field-induced fatigue was black. Note that the buzz always occurred and was independent of the crack length that would influence resonant frequency. Since the electric sparking was observed, it can be assumed that the electric breakdown occurred inside the crack. According the theory on electric breakdown [11], if there are bubbles in the liquid, since the electric fields in dielectrics under alternating current (AC) is inversely proportional to their permittivities, the electric field in the bubbles is always higher than that in the liquid. Because the electric field of electric breakdown in bubbles is less than that for liquid, the ionization

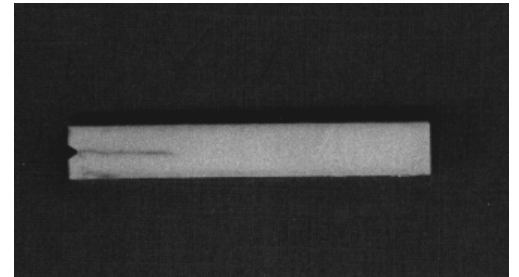


Fig. 2: The propagated macroscopic crack in the specimen

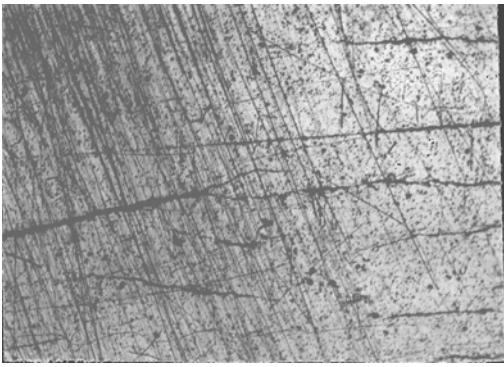


Fig. 3: Optical micrograph of a microcrack Distribution under $E=0.8E_c$ observed by microscopy with 50 multiplication.

Another important phenomenon was that crack growth has two patterns in ferroelectrics under electric cycling. One is the case of the low electric field, i. e. $E < 0.83E_c$, in which the macroscopic crack stoped growing after it grew a little bit, and many microcracks in front of the macroscopic crack tip were found by microscopy. Furthermore, these microcracks would grow with the increase of the cycling number. The microcrack distribution near the macro-crack is shown in Fig. 3. Another crack growth pattern is corresponding to

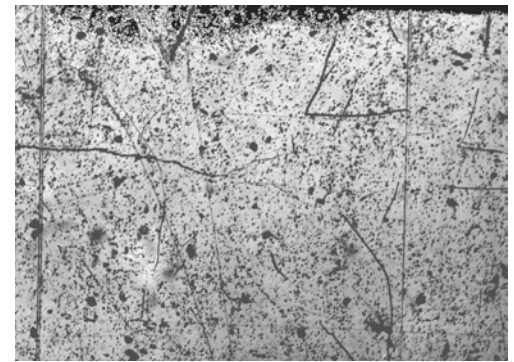


Fig. 4: Optical micrograph of a microcrack Distribution under $E=1.0E_c$ observed by microscopy with 50 multiplication.

the case of high electric field, i.e. $E > 0.83E_c$, in which only macroscopic crack propagated and no micro-cracks were found as shown in Fig. 4. It is believed that the propagation of the electric-field-induced fatigue crack depends on the competition between two mechanisms. That is, one results in macroscopic crack growth and the other leads to produce microcracks. When the electric field is low, the macroscopic crack grows very slowly, and the long period of time in the process permits microcracks to emerge and grow. On the other hand, the microcracks near the macroscopic crack tip would weaken the electric field and thus the macroscopic crack would grow more difficult. Finally, as well known, the micro-cracks will produce a shield that impedes the propagation of the macro-crack. But for the case of high electric field, since the macroscopic crack propagated rapidly, the

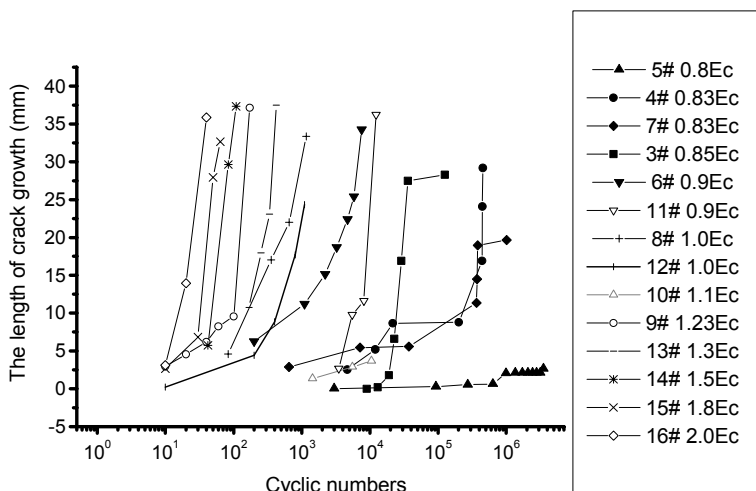


Fig. 5: Variation of crack growth length as a function of cyclic numbers

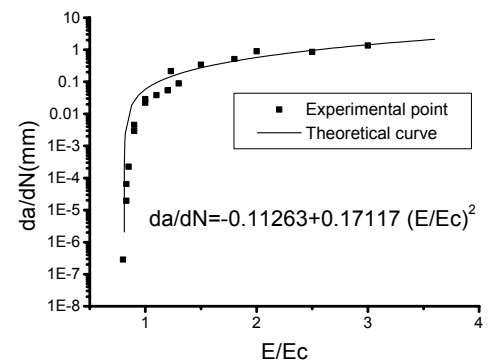


Fig. 6: Variation of crack growth rate as a function of electric field

Besides, the electric field at the back wakes of the macroscopic crack was weakened due to the existence of microcracks had no time to occur and grow.

would happen in the bubbles first, which would lead to both the increase of temperature and the inflation of the volume of bubbles. On the other hand, the ionization produces many electrons with high energy, which collides with the molecules of the liquid, makes the liquid ionize and produces more bubbles. With the growth and birth of the bubbles, the Bubble Bridge would finally be formed between the crack surfaces, and the electric breakdown would occur locally. Moreover, the electric breakdown occurred in the bubbles would get off light and sound. Therefore, the theory on electric breakdown can be used to explain the experimental phenomena including the occurrence of bubbles, the buzz, the black crack surfaces as well as the sparking.

the macroscopic crack, which can reduce the occurrence of microcracks as well. In Fig. 8, the curves between the loading numbers and the length of crack growth are presented. Note that although the crack growth rate varies significantly, they still almost are stable. The difference among the cyclic life corresponding to different amplitudes of the cyclic electric field can be considerably large. Fig.9 reveals the relationship between the electric loading and the crack growth rate. Although the logarithmic coordinate system is used, a nonlinear power relation between the electric field and the crack growth rate is obvious.

A THEORETICAL ANALYSIS OF THE CRACK GROWTH RATE

Fig. 7 shows the schematic of the proposed model.

A voltage is applied on the upper and lower surfaces of the specimen. Consider the energy release rate between two regions (region I and region II), as shown in Fig. 7. The region I denotes the region far behind the crack tip while the region II denotes the region far ahead of the crack tip. Since the region I and the region II are far from the crack tip, the mechanical and electrical fields are

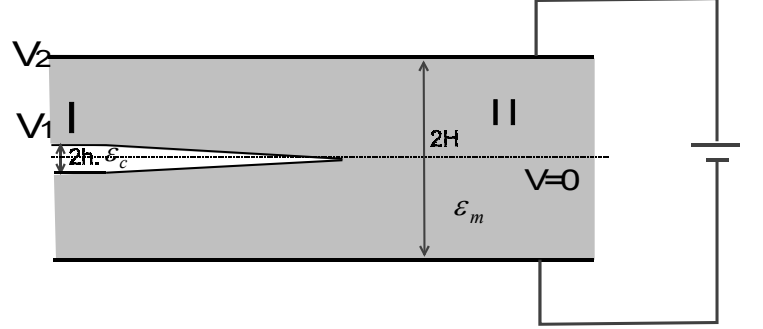


Fig. 7: Schematic of the analysis model

uniform in them. Note that the energy release rate for crack growth is the difference of the unit length energy between the region I and the region II. The voltage at the upper surface of the specimen is V_2 and the voltage at the upper crack surface in region I is V_1 . The height of the specimen is $2H$ and the distance between crack surfaces in region I is $2h$. The permittivities of the specimen and the medium inside the crack are ϵ_m and ϵ_c , respectively. Next, in order to calculate the energy of the region I and the region II, we define D_1 and D_2 as the electric displacements of the region I and the region II, respectively. Because the electric displacement vector in the region I or in the region II is perpendicular to the middle surface, only one component of the electric displacement vector is not zero and written as D_1 or D_2 . D_1 and D_2 can be calculated in the specimen subjected to an electric field as follows

$$D_1 = \frac{-V_2 \epsilon_c \epsilon_m}{\epsilon_m h + \epsilon_c (H - h)}, \quad D_2 = \frac{-V_2}{H} \epsilon_m \quad (1)$$

In order to calculate the total energy of unit length, the internal energy needs to be calculated at first. The internal energy of the region I and the region II is

$$U_1 = -V_2 D_1 = \frac{V_2^2 \epsilon_c \epsilon_m}{\epsilon_m h + \epsilon_c (H - h)}, \quad U_2 = -V_2 D_2 = \frac{V_2^2 \epsilon_m}{H} \quad (2)$$

The external force potentials of the region I and the region II are

$$F_1 = 2V_2 D_1, \quad F_2 = 2V_2 D_2 \quad (3)$$

The total energy of the region I and the region II is

$$\Pi_1 = U_1 + F_1 = V_2 D_1, \quad \Pi_2 = U_2 + F_2 = V_2 D_2 \quad (4)$$

From equation (1)-(4), the energy release rate can be obtained as

$$\begin{aligned} G = \Pi_2 - \Pi_1 &= V_2(D_2 - D_1) = V_2^2 \varepsilon_m \left(\frac{\varepsilon_c}{\varepsilon_m h + \varepsilon_c(H-h)} - \frac{1}{H} \right) \\ &= V_2^2 \varepsilon_m \frac{(\varepsilon_c - \varepsilon_m)h}{H[\varepsilon_m h + \varepsilon_c(H-h)]} \end{aligned} \quad (5)$$

From equation (5) one can know that only when $\varepsilon_c > \varepsilon_m$, the energy release rate, G , is positive. So if the crack is impermeable, that is $\varepsilon_c = 0$, the energy release rate is negative and it seems that the crack should not be able to grow. However, it has been found in the experimental observation that there exists the electric breakdown. Thus, if we assume that the crack is a conducting crack in the electric breakdown process, i.e. $\varepsilon_c \rightarrow \infty$, the energy release rate becomes positive. In addition, note that the total energy for the conducting crack is lower than one for the permeable crack and thus the energy difference makes the electric breakdown happen. Substituting $\varepsilon_c \rightarrow \infty$ into equation (5) we get

$$G = V_2^2 \varepsilon_m \frac{h}{H(H-h)} \quad (6)$$

From equation (6), we note that if h equals zero, i.e. corresponding to the case of a crack without width or a mathematical crack, the crack could not propagate. Actually, cracks always have finite width, and equation (6) shows that the greater h the higher energy release rate. From equation (6) it is found that the relationship between the driven energy for crack growth and the electric voltage or the electric field is $G \propto V^2 \propto E^2$. It can be assumed that the fracture resistance energy consists of two parts. One is G_1 , which represents the dissipated energy dependant on Δa (the crack growth in this step), and a further assumption of $G_1 \propto \Delta a$ is introduced. For example, the surface energy belongs to G_1 . The other part is G_0 , representing the dissipated energy independent of Δa or the least energy necessary to start fracture. The energy balance equation can be expressed as

$$AE^2 = G = G_1 + G_0 = B\Delta a + G_0 \quad (7)$$

where A and B are constants. From the above equation, we solve Δa as

$$\Delta a = -\frac{G_0}{B} + \frac{A}{B}E^2 = k_0 + k_1E^2 \quad (8)$$

where $k_0 = -\frac{G_0}{B}$ and $k_1 = \frac{A}{B}$ are constants to be determined. They can be obtained by fitting the experimental data as shown in Fig.6. In Fig. 6, the theoretically predicted curve is presented. It is found that there is a good consistence between test points and theoretical curve. Moreover, since $k_0 = -\frac{G_0}{B} < 0$ and $k_1 = \frac{A}{B} > 0$, it is known from equation (8) that there will be a critical electric field \tilde{E} which makes $\Delta a = 0$ and corresponds to the minimum value of the electric field that can make the crack grow. When $E < \tilde{E}$, Δa is negative, which means the crack could not propagate. The critical electric field can be obtained as $\tilde{E} \approx 0.81E_c$ from the theoretical curve presented in Fig. 6, which approximately equals to the experimental result. As shown in Fig. 5, when $\tilde{E} \approx 0.80E_c$, the cyclic number reaches four millions.

CONCLUSIONS

The electric-field-induced fatigue displays distinct characters under different magnitudes of electric loading. When $E < 0.83E_c$, the emergence and growth of microcracks is the major fatigue mechanism that impedes the macroscopic crack growing. Whereas, when $E > 0.83E_c$, the macroscopic crack growth is the dominant fatigue mechanism and no microcracks were found in experiments. The crack always propagates in company with the local electric breakdown occurred inside the crack. From the analysis, it is known that the electric field causes the positive energy release rate. The crack growth rate is nonlinearly related to the cyclic electric load.

REFERENCES

1. Furata A. and Uchino K. (1993) *J. Am. Ceram. Soc.*, 76:1615-1617.
2. Cao H.C., Evans A.G. (1994) *J. Am. Ceram. Soc.* 77:1783-1786.
3. Lynch C.S, Chen L., Suo Z., and McMeeking R.M., (1995) *J. of Intelligent Mater. Syst. And Struc.* 6:191-198.
4. Hill M.D., White G.S., Hwang C.S., Lloyd I.K. (1996) *J. Am. Ceram. Soc.* 79(7)1915-1920
5. Jiang Q.Y., Cross L.E. (1993) *J. Mater. Sci.* 28:4536-4543
6. Tai W.P. and Kim S.H. (1996) *Mater. Sci. and Engng.* B38:182-185
7. Zhu T., Fang F. and Yang W. (1999) *J. Mater. Sci. Letters* 18:1025-1027.
8. Winzer H., Schneider G.A., Steffens J., Hammer M. and Hoffman M.J. (1999) *J. of the European Ceramic Society* 19:1333-1337.
9. Zhang J.S., Dong Z.X., Hua X. and Fang D.N., (1999) *Proceedings of IMMM'99, the fourth International Symposium on Microstructures and Mechanical Properties of New Engineering Materials*, Beijing, International Academic Publishers, pp.121-125.
10. Park S. B. and Sun C. T. (1995) *J. Am. Ceram. Soc.* 78: 1475-1480.
11. Dwyer O' (1973) *The theory of electrical conduction and breakdown in Solid dielectrics*, Oxford: Clarendon Press.